

A Modified Quadratic Boost based P-type Structure with Inverting Output

P. Raviteja

Research Scholar
Electrical Engineering Department
National Institute of Technology
Warangal, Hanamkonda
pr22eer1r08@student.nitw.ac.in

K. Ashok kumar

Research Scholar
Electrical Engineering Department
National Institute of Technology
Warangal, Hanamkonda
ka719040@student.nitw.ac.in

M F Baba

Research Scholar
Electrical Engineering Department
National Institute of Technology
Warangal, Hanamkonda
mfbaba@student.nitw.ac.in

B L Narasimharaju

Professor
Electrical Engineering Department
National Institute of Technology
Warangal, Hanamkonda
blnraju@nitw.ac.in

A V Giridhar

Associate Professor
Electrical Engineering Department
National Institute of Technology
Warangal, Hanamkonda
giridhar@nitw.ac.in

Abstract— In This paper a modified quadratic boost converter (MQBC) based p-type structure with inverting output is presented. The proposed converter evolution based on integration of p-type converter structure and modified quadratic boost configuration. Output side inductor constitutes continuous output current. Main features of proposed MQBC converter are high voltage gain, continuous input current, inverting output which is used for LED driving, data transmission etc. In addition to that proposed converter has buck capability at duty ratio $D \geq 0.2929$. The detail description of proposed MQBC converter, steady state analysis, modes of operation, voltage and current stress analysis of semiconductor elements are presented in this paper. Further a 40/400 V, 300 W converter is validated with simulation results.

Keywords— DC-DC converter, High gain, Inverting output, non-isolated, Quadratic Boost.

I. INTRODUCTION

Now a days energy demand is more due to increased utilization of energy[1]. It causes the rise in generation of energy. Traditional sources of energy use coal, oil and uranium etc. which leads to pollution and deplete the natural resources. This can be avoided by using non-conventional energy sources (NCES) such as PV, wind, fuel cell and biomass etc. They need integration of DC-DC converters to step up or down the voltage levels based on the applications like portable electronic devices, LED lighting, dc micro grid. Based on the application DC-DC converters are buck, boost and buck-boost type. There are many DC-DC boost converters are proposed in the literature based on gain, isolation, non-isolated, coupled inductor. Isolated converters gives high voltage gain by using isolation transformer. Due to leakage flux in the isolated and coupled inductor [2], [3] based DC-DC boost converters introduces high voltage stress across semiconductor elements which results in high power losses. To avoid this, additional snubber circuitry is used which in turn causes increase in cost and size of converter.

Aforementioned drawbacks are mitigated by using non-isolated DC-DC converters. These converters are of high voltage gain, continuous input current, voltage stress is low and high efficiency obtained at reduced cost, size and weight. Conventional boost converter is simple in structure with less number of components but due to high voltage stresses across

semiconductor elements these are not apt for high power applications. Many non-isolated DC-DC high gain topologies are evolved in last decade like quadratic boost [4], [5], SEPIC, switched inductor, switched capacitor, cascaded, voltage multiplier, quasi Z source, hybrid switched inductor type. Few of the aforementioned converters achieve high voltage gain but contain more number of switches, diodes and energy storage elements, discontinuous input and output current. Those converters additional focus on performance enhancement.

To overcome the aforesaid limitations of converters by preserving the advantages MQBC is designed. The proposed MQBC is having advantages of simple structure, less number of energy storage elements compared to [6], continuous input and output current. The remaining paper is structured as follows: section II discusses about the steady state operation of proposed MQBC, section III presents the simulation results and section IV presents the conclusion.

II. STEADY STATE OPERATION OF PROPOSED MQBC

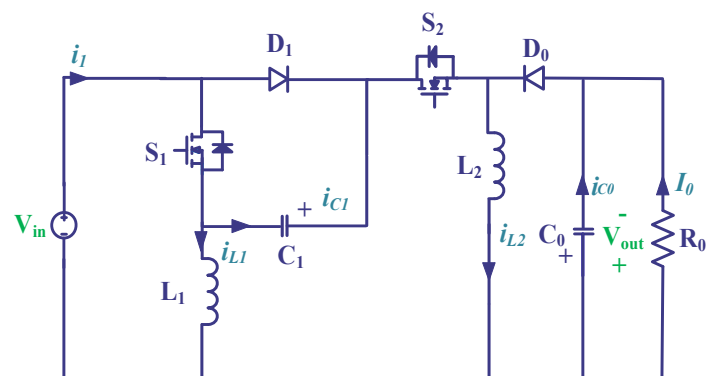


Fig.1. Proposed MQBC converter

The proposed MQBC converter shown in fig.1. The converter has two switches (S_1, S_2), two diodes (D_0, D_1), two inductors (L_1, L_2) and two capacitors (C_0, C_1). The Proposed BB converter operates in continuous conduction mode (CCM). All the devices used in the converter are assumed as ideal for the easier of analysis of converter in CCM. As shown in fig.2 MQBC converter operates in two modes. Typical waveforms of the converter are demonstrated in fig.3.

A. Modes of operation:

Mode-1 (t_0-t_1):

In this mode at $t=t_0$, as shown in fig.2. Mode 1, the S_1 , S_2 switches are turned ON and diodes D_0 , D_1 are in OFF state. The input DC source V_{in} is charges the inductor L_1 is and inductor L_2 is charged through the capacitor C_1 . The output load R_0 is supplied with the capacitor C_0 .

From Mode-1, in t_0-t_1 interval the following expressions are deduced by applying Kirchoff's voltage and current law.

$$\left. \begin{aligned} v_{L1} &= v_{in} \\ v_{L2} &= v_{in} + v_{C1} \end{aligned} \right\} \quad (1)$$

$$\left. \begin{aligned} i_{C1} &= C_1 \left(\frac{dv_{C1}}{dt} \right) = -i_{L2} \\ i_{C0} &= C_0 \left(\frac{dv_{C0}}{dt} \right) = -i_0 \end{aligned} \right\} \quad (2)$$

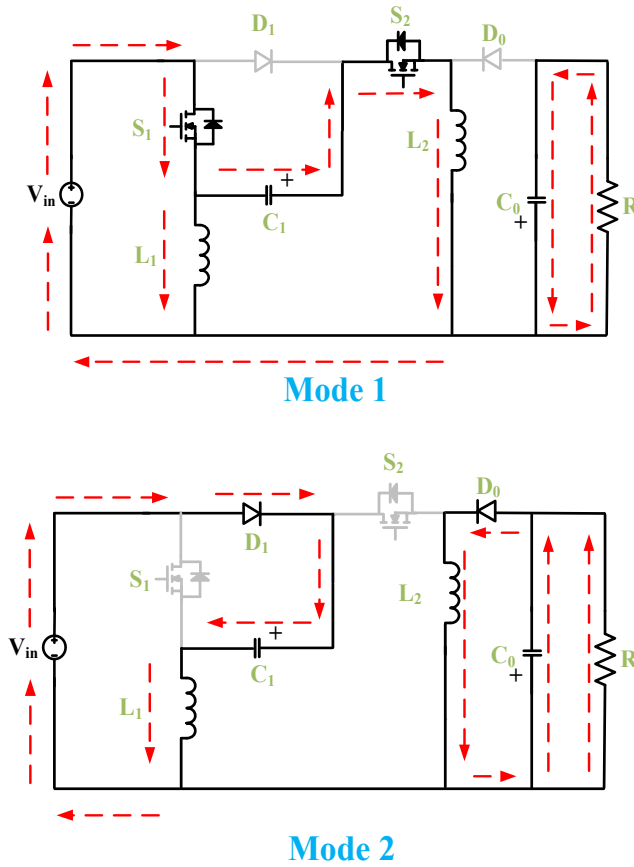


Fig.2. Modes of operation of MQBC converter

Mode-2 (t_1-t_2):

In this mode at $t=t_1$ the switches S_1 , S_2 are turned OFF, Consequently D_0 , D_1 diodes are in ON state as shown in fig.2. Mode 2. As compared with the previous mode inductors L_1 , L_2 are start discharging. Inductor L_1 discharged to charge the capacitor C_1 accompanied with the input DC source V_{in} . At the same time Inductor L_2 discharged to supply energy to output load R_0 and to charge the capacitor C_0 .

From Mode-2, in t_0-t_1 interval the following expressions are deduced by applying Kirchoff's voltage and current law.

$$\left. \begin{aligned} v_{L1} &= v_{in} - v_{C1} \\ v_{L2} &= -v_{out} \end{aligned} \right\} \quad (3)$$

$$\left. \begin{aligned} i_{C1} &= C_1 \left(\frac{dv_{C1}}{dt} \right) = i_{L1} \\ i_{C0} &= C_0 \left(\frac{dv_{C0}}{dt} \right) = i_{L2} - i_0 \end{aligned} \right\} \quad (4)$$

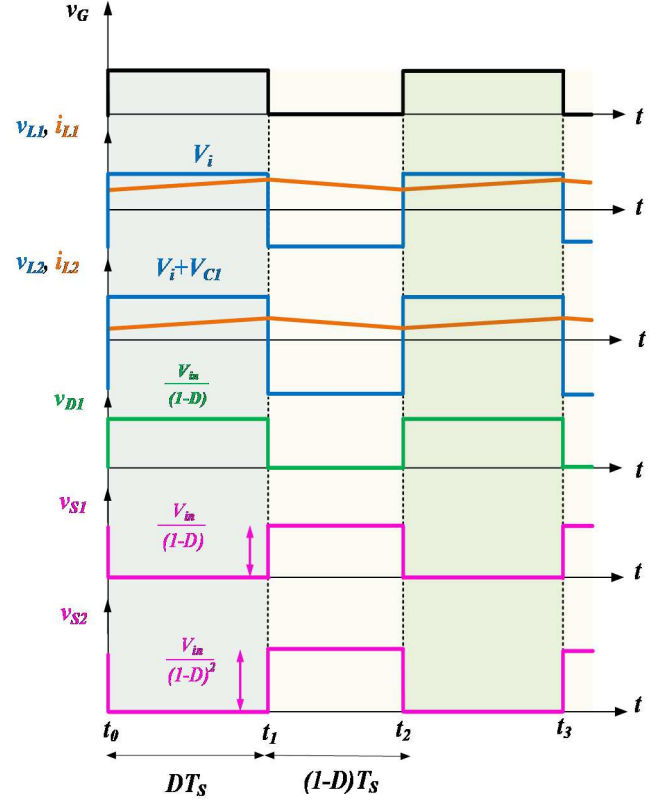


Fig.3. Typical waveforms of MQBC converter

Applying volt-sec balance on inductors L_1 and L_2 , the following equations are evolved.

$$(v_{in})D + (v_{in} - v_{C1})(1-D) = 0 \quad (5)$$

$$(v_{in} + v_{C1})D + (-v_{out})(1-D) = 0 \quad (6)$$

By solving (5) and (6) equations

$$v_{C1} = \frac{v_{in}}{1-D} \quad (7)$$

By using equation (7) output voltage gain of the proposed MQBC converter is given as

$$G \left(\frac{v_{out}}{v_{in}} \right) = \left(\frac{2-D}{1-D} \right)^2 \quad (8)$$

Similarly, by applying amp-sec balance on (2) and (4) the average inductor currents are represented as

$$\left. \begin{aligned} I_{L1} &= \frac{I_0 D}{(1-D)^2} \\ I_{L2} &= \frac{I_0}{(1-D)} \end{aligned} \right\} \quad (9)$$

B. Voltage and current Stress:

From modes of operation it can be noticeable that voltage and current stress [7] in semiconductor elements in proposed MQBC converter is given by

$$\left. \begin{aligned} V_{D1} &= v_{C1} = \frac{v_{in}}{1-D} = \frac{v_{out}(1-D)}{(2-D)D} \\ V_{D0} &= v_{L2} + v_{out} = \frac{v_{in}(2-D)}{(1-D)^2} = \frac{v_{out}}{(2-D)D} \\ V_{S1} &= v_{C1} = \frac{v_{in}}{1-D} = \frac{v_{out}(1-D)}{(2-D)D} \\ V_{S2} &= \frac{v_{in}}{(1-D)^2} = \frac{v_{out}}{(2-D)D} \end{aligned} \right\} \quad (10)$$

Average and peak current stresses of semiconductor elements are given by

$$\left. \begin{aligned} I_{S1} &= D(I_{L1} + I_{L2}) \\ I_{S2} &= DI_{L2} \\ I_{D1} &= (1-D)I_{L1} \\ I_{D0} &= (1-D)I_{L2} \end{aligned} \right\} \quad (11)$$

$$\left. \begin{aligned} \hat{I}_{S1} &= (I_{L1} + I_{L2}) + \left(\frac{\Delta I_{L1} + \Delta I_{L2}}{2}\right) \\ \hat{I}_{S2} &= I_{L2} + \left(\frac{\Delta I_{L2}}{2}\right) \\ \hat{I}_{D1} &= I_{L1} + \left(\frac{\Delta I_{L1}}{2}\right) \\ \hat{I}_{D0} &= I_{L2} + \left(\frac{\Delta I_{L2}}{2}\right) \end{aligned} \right\} \quad (12)$$

Where

$$\left. \begin{aligned} \Delta I_{L1} &= \left(\frac{V_{in}}{L_1}\right) \frac{D}{f_s} \\ \Delta I_{L2} &= \left(\frac{V_{in} + V_{C1}}{L_2}\right) \frac{D}{f_s} \end{aligned} \right\}$$

C. Design consideration:

(i) Inductor Design:

Inductors L_1, L_2 are designed based on the ripple current assumption of 20% to 40% ($\%X_{L1}$ & $\%X_{L2}$) of inductor average current.

$$\left. \begin{aligned} L_1 &\geq \frac{V_{in}D}{(\%X_{L1})I_{L1}f_s} \geq \frac{V_{in}^2(2-D)D}{(\%X_{L1})(1-D)^2P_o f_s} \\ L_2 &\geq \frac{(V_{in} + V_{C1})D}{(\%X_{L2})I_{L2}f_s} \geq \frac{V_{in}^2(2-D)^2D^2}{(\%X_{L2})(1-D)^2P_o f_s} \end{aligned} \right\} \quad (13)$$

(ii) Capacitor Design:

Capacitors C_0, C_1 are designed based on the admissible voltage ripple of 1% to 5% ($\%X_{C1}$ & X_{C0}) of respective capacitor average voltage.

$$\left. \begin{aligned} C_1 &\geq \frac{I_{C1}D}{(\%X_{C1})V_{C1}f_s} \geq \frac{P_o(1-D)^2}{(\%X_{C1})(2-D)D V_{in}^2 f_s} \\ C_0 &\geq \frac{I_{C0}D}{(\%X_{C0})V_{out}f_s} \geq \frac{P_o(1-D)^4}{(\%X_{C0})(2-D)^2D^2 V_{in}^2 f_s} \end{aligned} \right\} \quad (14)$$

D. Control Performance:

The performance evaluation of a Modified Quadratic Boost Converter (MQBC) is carried out by using the state-space averaging method [8]. This MQBC operates in two modes, as identified through steady-state analysis, which results in a set of differential equations for each mode.

The proposed MQBC topology has two inductors L_1, L_2 and two capacitors C_1, C_0 leading to four state variables: the currents $i_{L1}(t)$ and $i_{L2}(t)$ flowing through the inductors, and the voltages $v_{C1}(t)$ and $v_{C0}(t)$ across the capacitors. The control variable is $d(t)$ and voltage variables are $v_{in}(t), v_{out}(t)$. The small signal modelling is encapsulated in equations (15),(16).

$$\begin{aligned} A &= A_1D + A_2(1-D), \quad B = B_1D + B_2(1-D), \quad C = C_1D + C_2(1-D) \\ X &= -A^{-1}BU \\ F &= \{(A_1 - A_2)X\} + \{(B_1 - B_2)U\} \end{aligned} \quad (15)$$

$$A_1 = \begin{bmatrix} 0 & 0 & 0 & 0 \\ 0 & 0 & \frac{1}{L_2} & 0 \\ 0 & \frac{-1}{C_1} & 0 & 0 \\ 0 & 0 & 0 & \frac{-1}{R_0C_0} \end{bmatrix} \quad B_1 = \begin{bmatrix} \frac{1}{L_1} & \frac{1}{L_2} & 0 & 0 \end{bmatrix}^T$$

$$C_1 = [0 \quad 0 \quad 0 \quad 1]$$

$$A_2 = \begin{bmatrix} 0 & 0 & \frac{-1}{L_1} & 0 \\ 0 & 0 & 0 & \frac{-1}{L_2} \\ \frac{1}{C_1} & 0 & 0 & 0 \\ 0 & \frac{1}{C_0} & 0 & \frac{-1}{R_0C_0} \end{bmatrix}$$

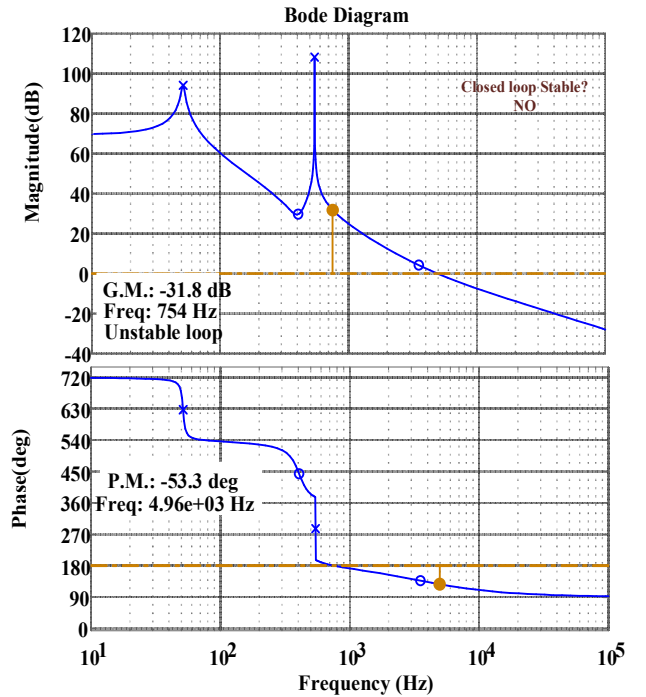
$$B_2 = \begin{bmatrix} \frac{1}{L_1} & 0 & 0 & 0 \end{bmatrix}^T$$

$$C_2 = [0 \quad 0 \quad 0 \quad 1]$$

$$\begin{bmatrix} \frac{di_{L1}(t)}{dt} \\ \frac{di_{L2}(t)}{dt} \\ \frac{dv_{C1}(t)}{dt} \\ \frac{dv_{C0}(t)}{dt} \end{bmatrix} = \begin{bmatrix} 0 & 0 & \frac{-(1-d)}{L_1} & 0 \\ 0 & 0 & \frac{d}{L_2} & \frac{-(1-d)}{L_2} \\ \frac{(1-d)}{C_1} & \frac{-d}{C_1} & 0 & 0 \\ 0 & \frac{(1-d)}{C_0} & 0 & \frac{-1}{R_0C_0} \end{bmatrix} \begin{bmatrix} \hat{i}_{L1}(t) \\ \hat{i}_{L2}(t) \\ \hat{v}_{C1}(t) \\ \hat{v}_{C0}(t) \end{bmatrix} + \begin{bmatrix} \frac{1}{L_1} \\ \frac{d}{L_2} \\ 0 \\ 0 \end{bmatrix} \hat{v}_{in}(t) + [F] \hat{d} \quad (16)$$

$$G_{vd} = \frac{\hat{v}_o(s)}{\hat{d}(s)} = \frac{-5.73 \times 10^{27} S^3 + 1.31 \times 10^{32} S^2 - 1.268 \times 10^{35} S + 8.243 \times 10^{38}}{2.267 \times 10^{23} S^4 + 4.25 \times 10^{24} S^3 + 2.678 \times 10^{30} S^2 + 4.894 \times 10^{31} S + 2.782 \times 10^{33}} \quad (17)$$

To ensure stable operation, a simple PI controller is implemented in resistant to variations of load current and input voltage. The controller adjust constant output voltage through specific gain $K_p=0.00000109$, $K_i=0.00331$. The closed loop stability of the proposed MQBC is validated through bode plots for both open and closed loop configuration as indicated in fig.4. (a), (b). Gain margin (G.M), Phase margin (P.M) values are also represented in the respective plots and also mentioned stability of the system. Proposed converter control to output transfer function is given in (17).



(a)

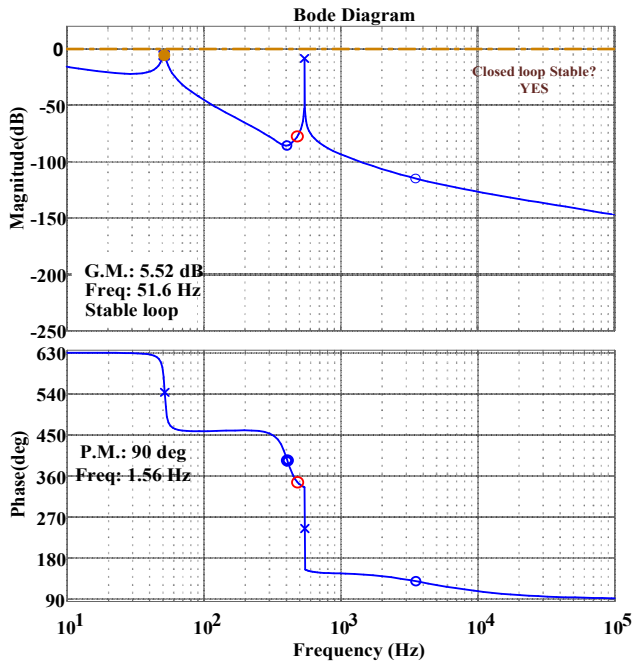
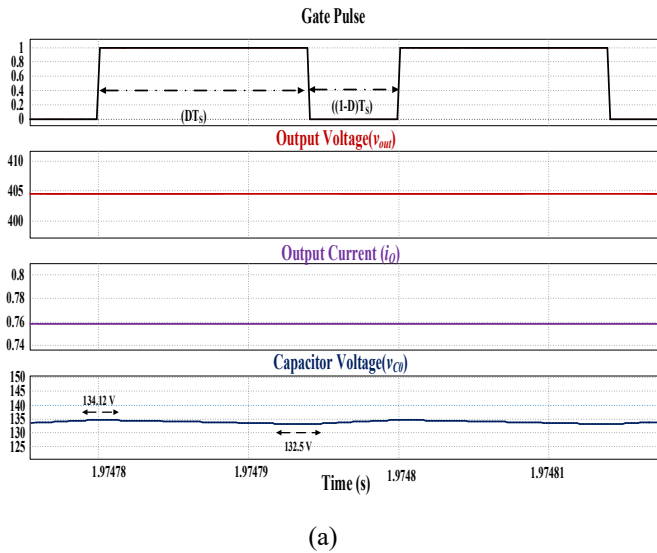


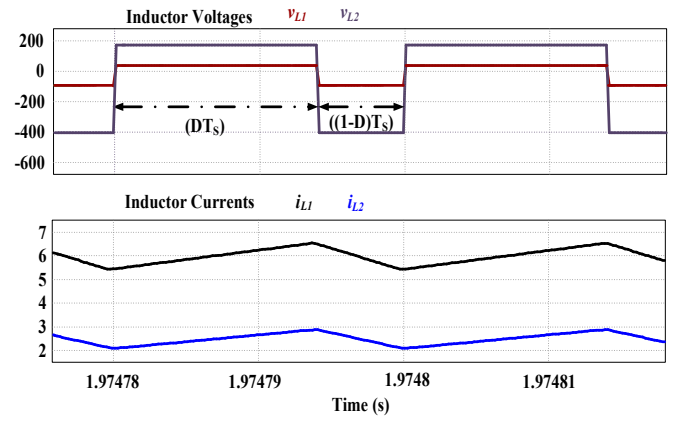
Fig.4. Bode plot of proposed MQBC: (a) open loop, (b) closed loop

III. SIMULATION RESULTS AND DISCUSSION

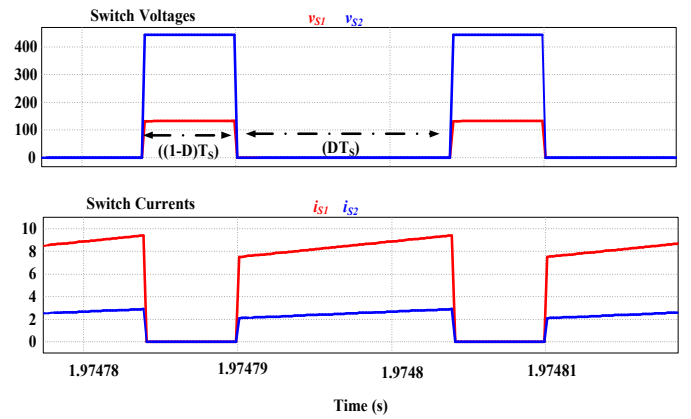
The proposed MQBC converter is authenticated by using simulation in PSIM platform. The proposed MQBC converter is supplied with input voltage of 40 V, duty cycle of 0.7 attains high gain of 10 times with output voltage of 400 V as shown in fig.4. (a). This clearly shows the voltage gain as in (8).



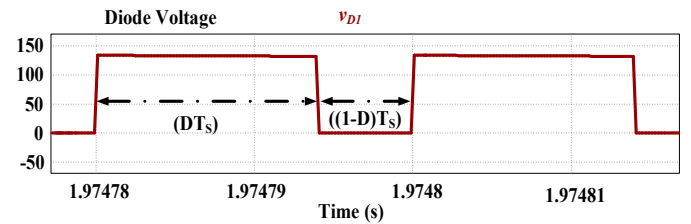
The next discussion is about the capacitor voltage V_{C1} , it has ripple content of 1.21% and the voltage ripple variation from 134.12 V to 132.5 V with average capacitor voltage of 133.31 V. The output current as shown in fig.4.(a) is of 0.75 A as is decided by the output voltage and power.



(b)



(c)



(d)

Fig.5. Simulation results (a) output voltage (v_{out}), current (i_o) and capacitor C_0 voltage (v_{C0}) (b) Inductor voltages and currents (c) Switch voltages and currents (d) Diode voltage

TABLE I. Simulation Circuit Parameters

Specification	Rating
Input voltage	40 V
Input current	7.5 A
Output voltage	400 V
Output current	0.75 A
Power rating	300 W
Duty	0.7
Inductors	$L_1=1\text{mH}, L_2=3\text{mH}$
Capacitors	$C_0=100\ \mu\text{F}, C_1=22\ \mu\text{F}$
Switching frequency	50kHz

The inductor voltages and currents of a proposed converter are satisfies (1), (2), and (9). As shown in fig.4. (b) it is found that inductor L_1 is selected with the less inductor current (i_{L1}) ripple is 9.7% and inductor L_2 is designed make converter in continuous conduction mode. As shown in fig.4. (c),(d) switches, diode voltage and current stresses validate (10) and (11). Voltage stress v_{S1} is across Switch S_1 is 130V and Voltage stress v_{S2} is across Switch S_2 is high i.e. 440V, because switch S_2 is at the output side so that it posed to high voltage stress. Simulation circuit parameters are given in Table I. Performance comparison of proposed converter is illustrated in Table II

TABLE II. Performance comparison

Ref	Proposed	Ref [6]	Ref [9]
Voltage gain	$\frac{(2-D)D}{(1-D)^2}$	$\frac{3}{(1-D)^2}$	$\left(\frac{D}{1-D}\right)^2$
Components (S/D/L/C)	2/2/2/2	1/6/2/3	1/5/3/3
Order	4	5	6
f/P	50kHz/300W	20kHz/300W	40kHz/130W
Voltage stress on Switch	$\frac{V_{in}}{1-D} \& \frac{V_{in}}{(1-D)^2}$	$\frac{V_{in}}{(1-D)^2}$	$\frac{V_{in}}{(1-D)^2}$
Voltage stress on Diode	$\frac{V_{in}}{1-D} \& \frac{V_{in}(2-D)}{(1-D)^2}$	$\frac{(1+D)V_{in}}{(1-D)^2}$	$V_{D1}=V_{D4}=\frac{V_{in}}{1-D}$ $V_{D2}=V_{D5}=\frac{DV_{in}}{(1-D)^2}$ $V_{D3}=\frac{V_{in}}{(1-D)^2}$
Polarity of Load Voltage	Inverting	Non-Inverting	Inverting

IV. CONCLUSION

In this paper a modified quadratic boost converter based on p-type structure with inverting output is introduced and validated with simulation. The converter performance is evaluated in continuous conduction mode (CCM). Modes of operation and voltage stress analysis and inductor, capacitor design, voltage stress analysis of semiconductor elements are explained in this paper. The proposed MQBC is having high gain of 10 and at duty ratio $D \geq 0.2929$ proposed converter behave as buck converter. From the performed analysis it is clear that MQBC is having continuous input current and inductor current ripple is less.

REFERENCES

[1] H. E. Murdock et al., "Renewables 2020-global status report," Int. At. Energy Agency, Vienna, Austria, Rep. INIS-FR-20-1110, Jun., 2020.

[2] B. L. Narasimharaju & Dubey, Pawan & Singh, S.P. (2012). Design and analysis of coupled inductor bidirectional DC-DC converter for high-voltage diversity applications. Power Electronics, IET. 5. 998-1007. 10.1049/iet-pel.2011.0141.

[3] Saeed Pourjafar, Hossein Madadi Kojabadi, Mohammad Maalandish, Mostafa Abarzadeh & Frede Blaabjerg (2020) Non-Isolated Coupled Inductor Based DC-DC Converter with High Voltage Conversion Ratio Recommended for Renewable Applications, Electric Power Components and Systems, 48:16-17, 1695-1707, DOI: 10.1080/15325008.2021.1908455.

[4] S. Rostami, V. Abbasi and M. Parastesh, "Ultrahigh Step-Up Non-Isolated DC-DC Converter Based on Quadratic Converter without Coupled Inductor," 2023 31st International Conference on Electrical Engineering (ICEE), Tehran, Iran, Islamic Republic of, 2023, pp. 154-159, doi: 10.1109/ICEE59167.2023.10334702.

[5] J. Leyva-Ramos, R. Mota-Varona, M. G. Ortiz-Lopez, L. H. Diaz-Saldierna and D. Langarica-Cordoba, "Control Strategy of a Quadratic Boost Converter With Voltage Multiplier Cell for High-Voltage Gain," in IEEE Journal of Emerging and Selected Topics in Power Electronics, vol.5,no.4,pp.1761-1770,Dec.2017,doi: 10.1109/JESTPE.2017.2749311.

[6] S. Mandal and P. Prabhakaran, "A Novel Non-Isolated Ultra High Gain DC-DC Converter with Single Switch and Dual Boost Cells," 2023 IEEE International Conference on Power Electronics, Smart Grid, and Renewable Energy (PESGRE), Trivandrum, India, 2023, pp. 1-6, doi: 10.1109/PESGRE58662.2023.10405162

[7] Baba MF, Giridhar AV, Narasimharaju BL. Active switched-capacitor based ultra-voltage gain quadratic boost DC-DC converters. Int J Circ Theor Appl. 2022;1 - 28. doi:10.1002/cta.3453

[8] M. F. Baba, A. V. Giridhar and B. L. Narasimharaju, "A Wide Voltage Range Bidirectional High Voltage Transfer Ratio Quadratic Boost DC-DC converter for EVs with Hybrid Energy Sources," in IEEE Journal of Emerging and Selected Topics in Industrial Electronics, doi: 10.1109/JESTIE.2023.3327639.

[9] N. Zhang, G. Zhang, K. W. See and B. Zhang, "A Single-Switch Quadratic Buck-Boost Converter With Continuous Input Port Current and Continuous Output Port Current," in IEEE Transactions on Power Electronics, vol. 33, no. 5, pp. 4157-4166, May 2018, doi: 10.1109/TPEL.2017.2717462.